Version of Record: https://www.sciencedirect.com/science/article/pii/S0169809520312047
Manuscript_6687958f1588dc31de78af6f98bfe906

Multiresolution decomposition and wavelet analysis of urban aerosol fluxes in Italy and Austria

Marianna Conte [1,*], Daniele Contini[1], Andreas Held[2]

[1]Istituto di Scienze dell'Atmosfera e del Clima, ISAC-CNR, Str. Prv. Lecce-Monteroni km 1.2, 73100 Lecce, Italy

[2] Environmental Chemistry and Air Quality, Department of Environmental Science and Technology, TU Berlin, Germany

*** Corresponding author**

Abstract

Observations of turbulent aerosol fluxes are fundamental to understand basic transport processes that govern changes of particle concentrations in the atmospheric boundary layer. The turbulent surface-atmosphere exchange of atmospheric particles can be quantified using several methods, including the eddy-covariance (EC) method and spectral flux estimation methods such as wavelet analysis and multiresolution decomposition. In this work, turbulent time series obtained by EC measurements in two different cities, Lecce (Italy) and Innsbruck (Austria), are spectrally analysed applying wavelet analysis and multiresolution decomposition, and the respective turbulent spectra are compared in these two European cities to quantify the contributions to turbulent fluxes in both the time and the frequency domains. As expected, particle emission is dominant in both cities following a similar diurnal cycle. Multiresolution decomposition reveals a similar cospectral peak of particle fluxes in both cities, with a median normalized frequency of n = 0.087 in Lecce and n = 0.086 in Innsbruck. Wavelet analysis shows that the 2 – 20 s time scales contribute very strongly to the particle flux in Lecce, while in Innsbruck the 20 – 200 s time scales are clearly dominant. In both cities, larger-sized eddies contribute only sporadically to turbulent aerosol fluxes. These results suggest that spectral similarity of urban particle number fluxes holds, to a large extent, even when comparing two very different urban environments and different meteorological conditions.

Keywords: Urban aerosol fluxes; spectral analysis; cospectral peak; spectral similarity, eddy-covariance.

Highlights

- Atmospheric particle emission is dominant in Lecce and Innsbruck
- The diurnal cycle of particle number concentrations is related with traffic activities
- Spectral similarity of urban particle number fluxes in both cities

Graphical abstract

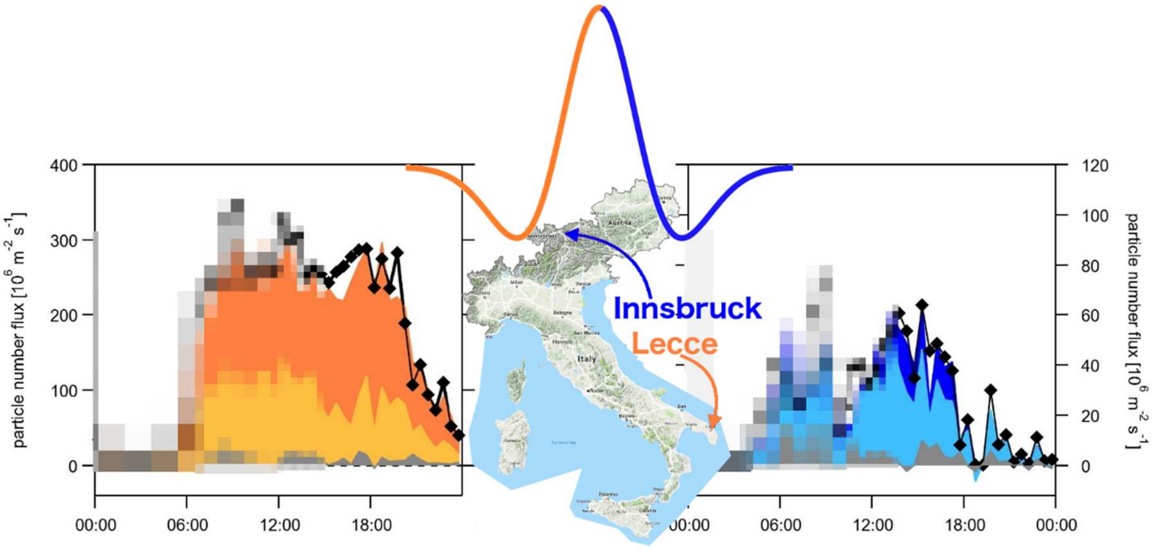

1 Introduction

Aerosols are continuously emitted from ground level sources and deposited back to the surface. Aerosol surface/atmosphere exchange is dominated by turbulent transport in so-called "eddies" (e.g. Reynolds, 1894; Foken, 2008). The net exchange is evaluated by measuring turbulent aerosol fluxes, representing a key process governing the atmospheric aerosol burden and its impact on climate, ecosystem health, and human health.

Our present knowledge of turbulent aerosol fluxes is incomplete, and thus, we lack a precise understanding of the transport processes that govern changes in atmospheric particle concentrations. The present paper aims to spectrally analyse turbulent time series and compare turbulent spectra in two different European cities, Lecce (Italy) and Innsbruck (Austria) using eddy covariance (EC; e.g. Aubinet et al., 2012) flux measurements. Wavelet analysis and multiresolution decomposition are applied to the EC data to compare co-spectra of atmospheric turbulent time series and quantify the spectral flux contributions. The importance of analysing data with wavelets lies in the time-frequency localization that allows to study features of the signal both in the time and the frequency domains.

The turbulent surface-atmosphere exchange of atmospheric particles is usually quantified with the EC method. This approach requires fast measurements of turbulent fluctuations of the vertical wind speed and aerosol concentration, typically with a measurement frequency of 10 Hz, under steady state conditions, i.e. negligible changes of the statistical properties of the vertical wind and aerosol time series during the measurement interval (typically 30 min). Then, turbulent particle fluxes are calculated as the covariance between the particle concentration and the vertical wind velocity. The first studies in urban areas were performed starting from the 2000s (e.g. Nemitz et al., 2000; Dorsey et al., 2002; Longley et al., 2004; Mårtensson et al., 2006; Martin et al., 2009).

Particle counters are typically not sufficiently fast for a measurement frequency of 10 Hz, and sudden changes in particle concentration inherently violate the steady state assumption. Therefore, due to limited instrument performance and non-ideal meteorological conditions, the post processing of EC particle flux data must include the application of corrections, e.g. for slow response of particle instrumentation, de-trending of time series, coordinate rotation of wind measurements, and rigorous quality assurance/control. To date, there is no best practice procedure for measuring the surface-atmosphere particle exchange, and no standard protocol for data processing and analysis. As an alternative to standard EC data processing, wavelet analysis is a spectral flux estimation method that, in contrast to EC, does not require the steady-state assumption. Even though spectral flux estimation methods such as wavelet analysis have been used to calculate turbulent fluxes (e.g. Katul and Parlange, 1995; Saito and Asanuma, 2008; van den Kroonenberg and Bange, 2007), these methods have barely been used with respect to particle fluxes.

The present work compares the meteorological conditions and turbulent fluxes in Lecce (Italy) and Innsbruck (Austria), and then analyse the source areas (footprints) of particle concentration and flux measurements to estimate the contribution of different source areas to the measurement. After a comparison of diurnal cycles of meteorological parameters and turbulent fluxes, multiresolution decomposition is applied in order to compare normalized cospectra of particle number and buoyancy fluxes and their diurnal evolution, and quantify the normalized frequency of the cospectral peak. Finally, wavelet analysis is applied to extract the dominant time scales of the turbulent fluxes, and to spectrally estimate 1 min particle number flux averages. The overall aim of this study is to characterize the temporal dynamics of particle fluxes in two different cities with high resolution both in the time and frequency domains.

2 Sites and methods

2.1 Measurement sites and experimental setup

Turbulent aerosol fluxes from two different cities, Innsbruck (Austria) and Lecce (Italy), were compared. The measurements were carried out between 10 March and 24 April 2015 in Lecce, and between 27 July and 21 August 2015 in Innsbruck. Both of the experimental sites, Innsbruck and Lecce, were located on the rooftop of university buildings within the respective city centres.

Innsbruck is situated in the Alpine Inn Valley, with a population of about 130000 inhabitants. The Innsbruck site (Karl et al., 2020; latitude 47°15′51.50″ N; longitude 11°23′6.77″ E) is located south west of the city centre, and it is characterized by a mountain-valley wind system (Deventer et al., 2018; von der Heyden et al., 2018). The prevailing wind direction during the measurement period was ENE, and the maximum wind speed was 7.8 m s^{-1} (Fig. 1a). The Innsbruck site is surrounded by office and commercial areas, close to the Inn river and close to a busy state road (B171 “Innrain”) where vehicular traffic reached a maximum of 650 vehicles per hour. The measurements for this study were carried out with a sonic anemometer (CSAT3, Campbell Scientific Inc., Logan, USA) and a Condensation Particle Counter (CPC, Model 3772, TSI Inc., Shoreview, USA).

Lecce is situated in South-Eastern Italy close to the sea, with a population of about 95000 inhabitants. The Lecce site (latitude 40°21’22’’N; longitude 18°10’02’’E) is located in a street called “student’s street” for the high presence of schools and university buildings, and where traffic reached a maximum of 2400 vehicles per hour. The main wind direction during the experimental campaign was N and the maximum wind speed was 5.4 m s^{-1} (Fig. 1b). The experimental setup for this study comprised an ultrasonic anemometer (Gill R3-100, Gill Instruments, Lymington, UK) coupled with a CPC (Grimm 5.403, Grimm Aerosoltechnik, Ainring, Germany).

The two sites exhibit several characteristic differences, including (1) the geographical and topographical conditions, (2) the experimental setup, and (3) the surface properties. First, the street-level elevation at the Innsbruck site is 570 m above sea level, i.e. much higher than at the Lecce site at 55 m above sea level. Innsbruck is situated in the Inn valley that represents the transition zone from Mediterranean to continental climate, while the Lecce site is about 12 km from the coastline of the Adriatic Sea. Second, the eddy-covariance instrumentation was located on the roof of a university building for the Innsbruck and Lecce sites at a height above ground level of 38.6 m and 14 m, respectively. Furthermore, to minimize potential flow distortions due to the presence of high buildings surrounding the sites, a wind sector between 140° and 190° was discarded from the Innsbruck data (leaving 90 % of the total measurements), and a sector from 20° to 202° was eliminated from the Lecce data (leaving 59 % of the total measurements). The first-order time constant of the CPC, used in the Lecce site, was determined by estimating in laboratory the time response to a concentration step. The results obtained in several repeated laboratory experiments was 1.3±0.05 s (Conte et al., 2018). The size range of the instrument is between 0.009 µm and 0.25 µm. At the Innsbruck site, the CPC has a nominal size range between 0.010 µm and > 1 µm, and the experimentally determined response time was 0.46 s (von der Heyden et al., 2018). Third, to characterize the surface properties of the urban canopies, the zero-plane displacement height (d_0) and the roughness length (z_0) parameters were evaluated for both sites. These parameters were evaluated for Lecce using a fitting of measured EC data under unstable conditions (Toda and Sugita, 2003). The value of d_0 was derived from the standard deviation of temperature and of vertical wind speed; the value of z_0, instead, was derived from a wind profile equation including the derived d_0 value. These values were estimated to be $d_0 = 7$ m and $z_0 = 1.3$ m (Conte et al., 2018). For Innsbruck, the parameters were evaluated with a height-based morphometric method (Grimmond and Oke, 1999), a mean building height of $z_B = 20$ m, $d_0 = 0.7z_B$, and $z_0 = 0.1z_B$. The values were estimated to be about $d_0 = 14$ m and $z_0 = 2$ m (von der Heyden et al., 2018).

2.2 Source area analysis

Source area (footprint) analysis is important to estimate the pollutants' relative weights at the measurement point. A source area is defined as the fraction of the surface containing effective sources and sinks contributing to the measurement point (e.g. Schmid and Oke, 1990; Kljun et al., 2002). In this study, the source area for particle concentrations and fluxes was determined as the characteristic dimension of the oval-shaped area representing 50 % of measured concentrations or fluxes. Following Schmid (1994), the parameters defining the shape of the source areas were evaluated analytically by two equations that represent the normalised source area dimensions, D_N. The source areas depend on the measurement height (z_m), and surface-layer scaling parameters such as the surface roughness length (z_0), the Obukhov length (L), the standard deviation of lateral wind speed fluctuations (σ_v), and the friction velocity (u_*):

$$D_N = \alpha_1 (\frac{z_m}{z_0})^{\alpha_2} \exp\left[\alpha_3 \left(\frac{z_m}{L}\right)^{\alpha_4}\right] \left(\frac{\sigma_v}{u*}\right)^{\alpha_5} \quad \text{(stable cases)} \quad (1)$$

$$D_N = \alpha_1 (\frac{z_m}{z_0})^{\alpha_2} \exp\left[1 - \alpha_3 \left(\frac{z_m}{L}\right)^{\alpha_4}\right] \left(\frac{\sigma_v}{u*}\right)^{\alpha_5} \quad \text{(unstable cases)} \quad (2)$$

The parameters α_i (i=1,5) referring to two types of equation, are numerical inputs evaluated separately for stable (equation 1) and unstable (equation 2) conditions according to the tables given in Schmid (1994). The numerical values α_i differ for concentrations and fluxes and determine the elliptical shape of the source areas. In this work, the oval-shaped source areas were approximated by ellipses oriented along the wind direction. For every 30-min period, a function was defined, equal to one inside the elliptical domain and equal to zero outside the elliptical domain: the source area is finally the sum of all these functions normalized by the total number of measurements.

2.3 Flux calculation and spectral analysis

The EC data from Innsbruck and Lecce were studied applying wavelet analysis and multiresolution decomposition in order to investigate the temporal dynamics of particle fluxes in detail. The EC method is commonly used to calculate vertical turbulent fluxes between surfaces and the atmosphere. It requires fundamental assumptions such as steady state conditions and horizontal homogeneity (e.g. McMillen 1988; Foken & Wichura, 1996).

The EC method expresses a turbulent flux F_{EC} of a certain entity by the covariance between the concentration *c* of that entity and the vertical wind velocity *w*:

$$F_{EC} = \overline{c'w'} \quad (3)$$

where the prime (′) denotes the fluctuating part of that entity. Equation 3 represents the turbulent vertical transport of *c* by fluctuations of *c* and *w* around their mean values (Baldocchi et al., 1988; Arya, 1999; Burba et al., 2012). The advantage of this method consists in the direct and in situ flux measurement without perturbation of the analysed ecosystem (Aubinet et al., 2012). An averaging period of 30 minutes is typically chosen. However, the 30-minute data obtained from EC need an accurate quality check and consistent post-processing. While the three-dimensional wind measurements using sonic anemometers are expected to be fully resolved at the sampling frequency of 10 Hz, the particle concentration measurements are dampened with experimentally determined response times of 1.3 s for the CPC used in Lecce, and 0.46 s for the CPC used in Innsbruck. The expected reduction of the EC flux estimate due to imperfect sensor response can be taken into account as proposed by Horst (1997). To minimize the impact of the imperfect sensor response on the comparison of EC flux calculations and spectral analyses, all following calculations in this study are based on 1 Hz data sets. The quality of the final data is mainly influenced by sensor configuration, by meteorological conditions, and depending on the validity of the steady state assumption (Foken & Wichura, 1996; Moncrieff et al. 1996, Aubinet et al., 1996).

A method which does not rely on the steady state assumption to evaluate the turbulent flux is the wavelet approach (e.g. Torrence and Compo, 1998; Schaller at al., 2017). The total flux $F_{Wavelet}$ is the integral of the cross-wavelet spectrum E_{cw} between the particle concentration *c* and the vertical wind velocity *w*, and can thus be computed as:

$$F_{\text{Wavelet}} = \delta j \sum_{j=0}^{J} \frac{E_{cw}(j)}{s_j} \qquad (4)$$

Equation (4) represents the sum over all scales s_j of the real part of the cross-wavelet spectrum E_{cw}, and δj is the scale step size. The cross-wavelet spectrum is defined as:

$$E_{cw}(j) = \frac{\delta t}{R}\frac{1}{N}\sum_{n=0}^{N-1}[W_n^c(s_j)(W_n^w(s_j))^*] \qquad (5)$$

where $W_n^{c,w}(s_j)$ are the wavelet transforms of the time series of *c* and *w*, respectively, and the asterisk (*) indicates the complex conjugate of the wavelet transform, δt is the time step of the time series, R is a reconstruction factor specific to the applied wavelet (e.g. R = 3.541 for the Mexican Hat wavelet, cf. Torrence and Compo, 1998), and N is the number of data points of the time series in the averaging period. It is useful to recall that the wavelet transform of a generic discrete time series $x_n(t), n = 0, \ldots, N-1$ is generally defined as the convolution of the series with a scaled "s" and time-shifted wavelet function ψ(t):

$$W_n(s) = \sum_{n'=0}^{N-1} x_{n'}(t) \times \Psi^*\left(\frac{(n-n')\delta t}{s_j}\right) \qquad (6),$$

allowing to obtain information about variability both in time and frequency of the time series. For further details see Torrence and Compo (1998) and Schaller at al. (2017).

The scales "s_j" entering in the equations (4) - (6) are typically conveniently chosen as fractional powers of two:

$$s_j = s_0 2^{j\delta j} \quad (7)$$

with j = 0 to the maximum number of scales J, the smallest resolvable scale $s_0 = 2\delta t$, and the scale step size δj, in this study set to 0.25. The wavelet function is chosen according to the characteristics of the time series. In this study, the Mexican Hat wavelet was used to obtain the wavelet transforms of the two time series, $W_n^2(\mathrm{s})$, and information about the contribution of different frequency and time domains to the cross-wavelet spectrum. Thus, it is possible to evaluate turbulent fluxes over short averaging intervals, e.g. 1 min flux estimates.

The data collected during both experimental campaigns were processed also using the multiresolution flux decomposition method (MRD). This analysis allows to decompose a time series $x_n(t)$ into averages on different time scales, obtained by M subsequent divisions of the whole time series starting from coarse (the whole series) to finer divisions in 2^M averaging points. This procedure of averaging using different window lengths corresponds to viewing the data at different resolutions, with each mode of the multiresolution decomposition corresponding to a certain moving average with a given length (Howell and Mahrt 1995):

$$\overline{x_n}(2^m) = \frac{1}{2^m} \sum_{i=(n-1)2^m+1}^{n2^m} x_i \quad (8)$$

where n=1,2,….,2^{M-m} is the window and x_i denotes the "residual" of the time series, that is the difference between the series and its approximation of order n. Once the temporal series is transformed by MRD in a frequency series, considering again the concentration *c* and the vertical wind velocity *w,* it is possible to evaluate the turbulent flux F_{MRD}:

$$F_{MRD} = \sum_{m=1}^{M} \frac{1}{2^{M-m}} \sum_{n=1}^{2^{M-m}} (2^{m-1}\overline{c_{2n}} - 2^m\overline{c_n})(2^{m-1}\overline{w_{2n}} - 2^m\overline{w_n}) \quad (9)$$

The three methods, EC, wavelet and MRD, allow to evaluate turbulent fluxes of a certain quantity. The EC method allows to investigate a turbulent flux on the ecosystem scale but it does not allow to obtain information about short-time turbulent events due to a violation of the steady state assumptions, on which this method is based. To overcome the steady-state requirement of EC, the wavelet analysis provides a localization, and thus a detailed analysis, of the turbulent events in both time and frequency. Wavelet analysis can provide the variability of a specific turbulent event and how its variability changes in time (Torrence and Compo 1998). MRD can be defined as nonoverlapping spectral analysis that provides information about the time scales of atmospheric fluctuations of a certain scalar. MRD typically has a smaller resolution in the frequency domain than wavelet analysis. The MRD locally decomposes the turbulent flux trying to characterize the dominant local events that correspond to the different averaging lengths considered in the analysis.

3 Results

3.1 Overview of campaigns in Lecce and Innsbruck

General overview

Figure 1 and Table 1 summarize the time series, median values, and 5 % and 95 % percentiles of meteorological data and particle concentrations and fluxes in the Lecce and Innsbruck measurement campaigns. Due to the earlier time of year, the range of the air temperature (Fig. 1) and the median air temperature is lower during the Lecce campaign in March and April 2015 than during the Innsbruck campaign in July and August 2015. In both locations, wind speed exhibits a clear diurnal cycle with calm nights and higher wind speeds during the day. The median wind speed of 1.8 m s^{-1} is slightly larger in Lecce than in Innsbruck (median wind speed 1.1. m s^{-1}), however, a southerly Foehn event in Innsbruck on 23 and 24 August is the reason for higher maximum wind speeds in Innsbruck. The prevailing wind direction during the Lecce campaign is from the North, while the Innsbruck campaign is characterized by a pronounced mountain-valley wind system with wind from the ENE during the day and from the SW at night. This regular change of wind direction in the Inn valley typically occurs between 09:30 and 11:00 in the morning, and between 17:30 and 19:00 in the evening. While the baseline particle number concentration (5 % percentile) of roughly 4000 cm^{-3} is similar in Lecce and Innsbruck, the median and the 95 % percentile values of particle number concentration are considerably larger in Lecce (median: 11419 cm^{-3}) than in Innsbruck (median: 8990 cm^{-3}). Similarly, the particle number fluxes are larger in Lecce than in Innsbruck, and the fraction of positive particle number fluxes, i.e. net particle emission, is considerably larger in Lecce (90.6 %) than in Innsbruck (69.7 %) as well. The buoyancy flux reaches larger maximum values in Lecce than in Innsbruck. The stability conditions are mostly near-neutral ($|z_e/L| < 0.1$, where $z_e=z-d_0$ is the effective measurement height) or slightly unstable in Lecce, while unstable conditions ($z_e/L < -0.1$) prevail in Innsbruck.

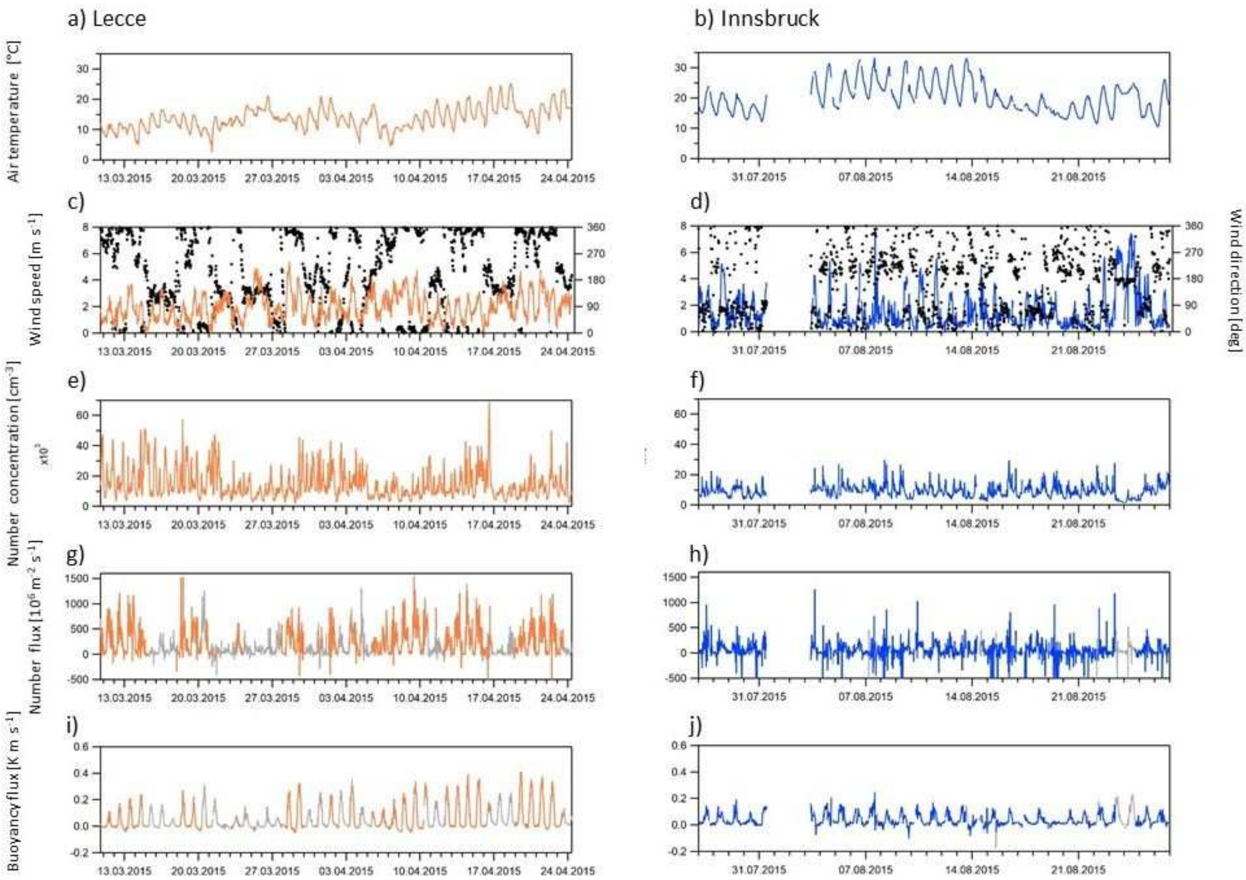

Fig. 1: Time series of a,b) air temperature, c,d) wind speed (continuous line) and wind direction (dots), e,f) particle number concentration, g,h) particle number flux, i,j) and buoyancy flux of the measurement campaigns in Lecce and Innsbruck; grey flux data are from discarded wind sectors.

Tab. 1: Median values and 5 % and 95 % percentiles of air temperature, wind speed, particle number concentration, particle number flux, friction velocity u*, buoyancy flux, and stability parameter z_e/L (Obukhov length $L = -\frac{u^{*2}}{k\left(\frac{g}{T_0}\right)T_*}$, where k is von Kármán constant, g $/T_0$ is a buoyancy parameter and T* is the friction temperature) of the measurement campaigns in Lecce and Innsbruck.

	Lecce			Innsbruck		
	5 %	median	95 %	5 %	median	95 %
air temperature [°C]	8.3	13.5	20.5	13.3	19.6	29.8
wind speed [m s^{-1}]	0.6	1.8	3.8	0.3	1.1	4.6
particle number concentration [cm^{-3}]	4336	11419	34983	3826	8990	17151
particle number flux [10^6 m^{-2} s^{-1}]	-14.9	210.8	789.8	-209.4	40.2	307.2
u* [m s^{-1}]	0.12	0.44	0.84	0.10	0.24	0.52
buoyancy flux [K m s^{-1}]	-0.02	0.01	0.28	-0.01	0.02	0.12
z_e/L [-]	-0.2	0.0	0.1	-7.0	-0.7	0.2

Source area estimates

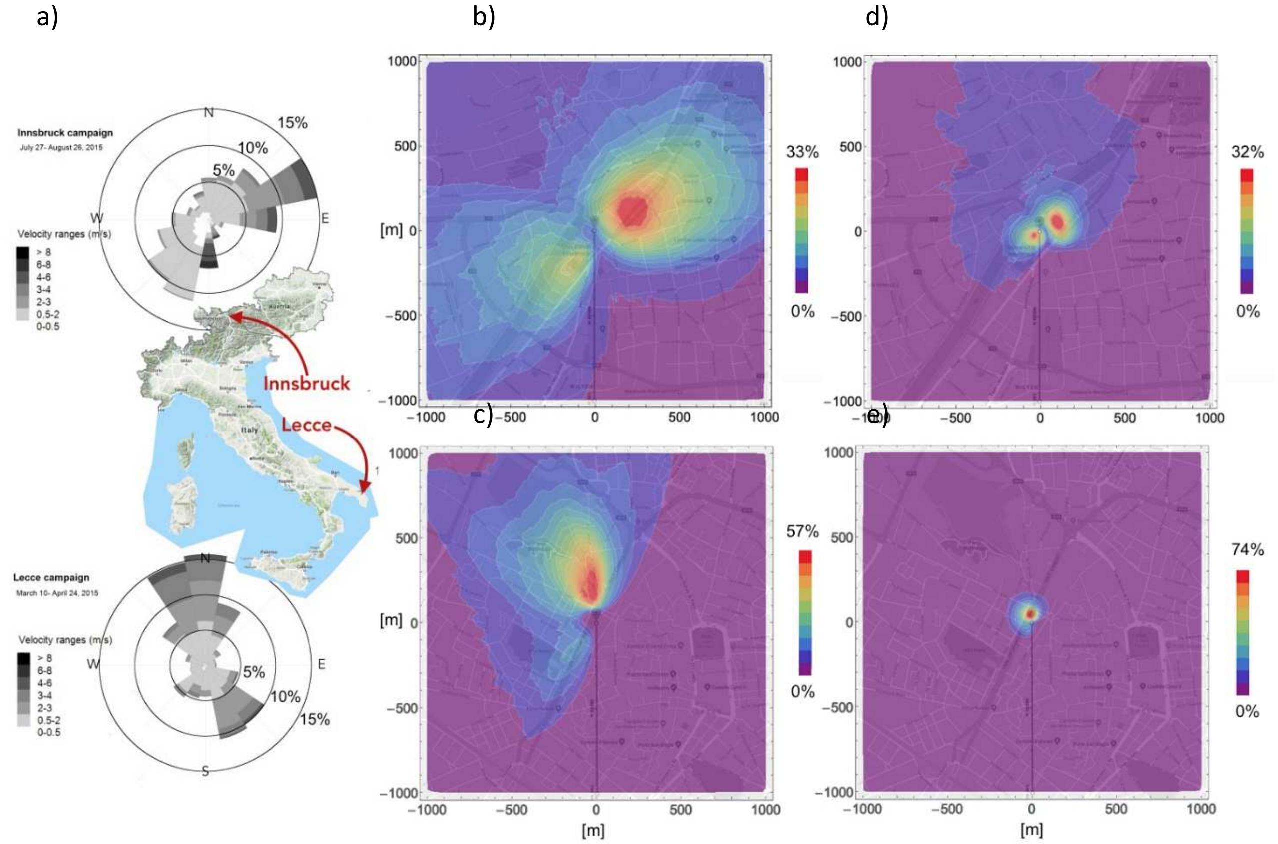

Figure 2: a) Location and wind roses of the measurement sites in Innsbruck and Lecce, as well as average concentration source areas (b, c) and average flux source areas (d, e). The color scale represents the percentage of measures that gives contribution to the source area in any point.

The source area estimates calculated using Eqs. 1 and 2 (section 2.2) are reported in Figure 2b and 2c for concentrations, and in Figure 2d and 2e for fluxes, for Innsbruck and Lecce, respectively. In Innsbruck, the dominant concentration source areas are to the N/NE with the densely built old town including a state road and public transportation to the city centre, and to a lesser extent to the SW with University buildings and residential areas. The Innsbruck flux footprint is mostly affected by the nearby University buildings in the S/SW sector. In Lecce, the dominant concentration and flux source areas are to the North of the measurement site with many buildings and roads with a high traffic density. The colour scale ranges from red, corresponding to the most influential areas, to blue for the areas minimally influencing the measurements. Normalized over all measurement periods, the most influential areas with respect to concentrations (red colours in Fig. 2b,c) are about 24 % and 55 % of the average source area in Innsbruck and Lecce, respectively, while the areas of minimum influence (blue colours) are about 2 % and 5 % of the average source area. For fluxes (Fig. 2d,e), the most influential areas are 10 % of the average flux source area in Innsbruck, and 12 % in Lecce, while the minimum influential areas are about 1 % of the average flux source area in both cities. In general, source areas for fluxes are smaller than those for concentrations (Contini et al., 2012; Vesala et al., 2008; Conte et al., 2018) because their values are proportional to the difference between particles crossing the measurement level in upward and downward direction (Vesala et al., 2008), whereas particles crossing the measurement point always contribute positively to the evaluation of concentration source areas. Furthermore, flux measurements consider only the turbulent transport of a scalar, while concentration measurements consider also transport by the mean flow.

Diurnal cycles

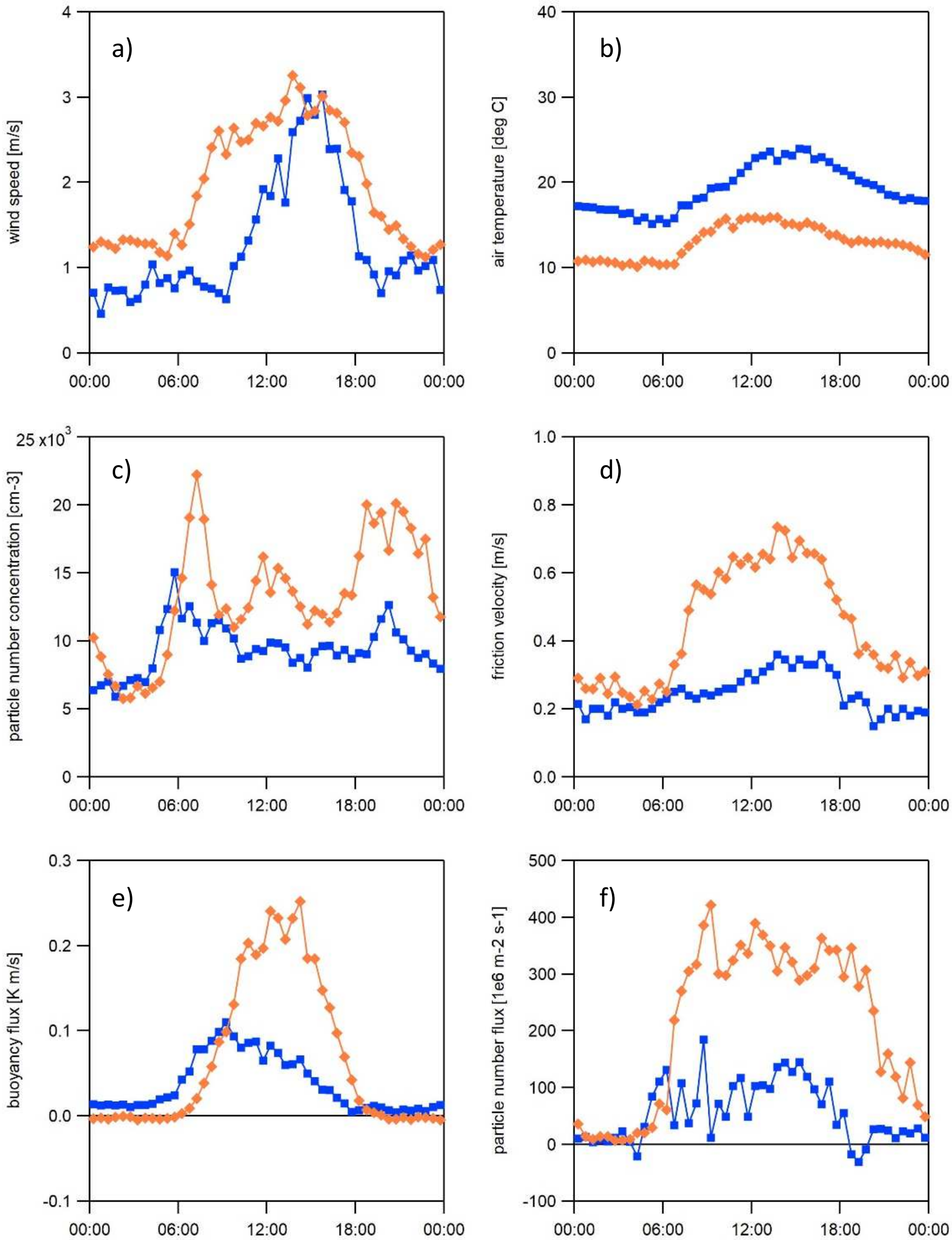

Fig. 3: Median diurnal cycles of (a) wind speed, (b) air temperature, (c) particle number concentration, (d) friction velocity, (e) buoyancy flux, and (f) particle number flux in Lecce (orange) and in Innsbruck (blue); EC data after "bad" wind sectors removed.

Figure 3 shows median diurnal cycles of wind speed, air temperature, particle number concentration, friction velocity, buoyancy flux, and particle number flux obtained by EC method in Lecce (orange) and Innsbruck (blue). As mentioned before, there is a clear diurnal cycle of wind speed (Fig. 3a) with calm nights and higher wind speeds during the day, from about 06:00 to 21:00 in Lecce and from about 09:00 to 20:00 in Innsbruck. The peak wind speed of about 3 m s^{-1} is reached in the afternoon between 13:00 and 16:00 at both sites. The diurnal cycle of air temperature (Fig. 3b) is very similar but shifted to higher temperatures in Innsbruck during the summer season. Temperatures begin to rise at 07:00 in the morning at both sites. Particle number concentrations (Fig. 3c) show several peaks during the course of the day: First, at both sites there is a steep increase in particle number concentration from 04:30 in the morning reaching the peak value of 15000 cm^{-3} in Innsbruck at 06:00, and 22000 cm^{-3} at 07:00 in Lecce. A second, slightly lower peak can be observed at both sites in the evening hours around 21:00. Only in Lecce, a clear third peak is found around noontime in correspondence of the maximum in solar radiation. Since the central peak happens around midday at noon, in correspondence of the maximum in solar radiation, it was possible that this increase in concentrations was related to local nucleation. The absence of this central peak in the suburban environment excluded a regional nucleation process pointing to an urban nucleation event. The presence of this peak in the Lecce data set has already been discussed by Conte et al. (2015) and Conte et al. (2018). This feature cannot be found in the Innsbruck data.

The friction velocity (Fig. 3d) is clearly enhanced during daytime both in Lecce and in Innsbruck, which indicates well-developed turbulent conditions. The median friction velocity in Lecce is between 0.6 and 0.8 m s^{-1} from 08:00 to 18:00, while the peak median friction velocity in Innsbruck is much lower, around 0.3 m s^{-1} from 11:00 to 18:00. The buoyancy flux (Fig. 3e) is mostly positive and exhibits a clear diurnal cycle with values close to zero during the night, and an increase after sunrise, which occurs earlier in the Innsbruck summer data (July/August) compared to the Lecce data from March/April. Again, the peak median buoyancy flux in Lecce is more than double compared to the Innsbruck peak value. Both in Lecce and Innsbruck, the median buoyancy flux drops back to values close to zero in the evening around 18:00. The particle number fluxes (Fig. 3f) are mostly positive both in Lecce and in Innsbruck, indicating net particle emission especially during the day. From 00:00 to 04:00 the net particle number fluxes are close to zero, and start to increase at the same time when particle number concentrations increase. During daytime, median particle number fluxes in Lecce are between 300 and $400 \cdot 10^6$ m^{-2} s^{-1}, while the median particle number fluxes in Innsbruck are between 50 and $150 \cdot 10^6$ m^{-2} s^{-1}. Interestingly, in Innsbruck there is a brief period of net particle deposition in the evening from 18:30 to 20:00, which cannot be observed in Lecce.

Adding data from the "bad" wind sectors does not considerably change the diurnal cycles in Innsbruck with respect to wind speed, air temperature, particle number concentration, and friction velocity but it slightly decreases the median estimates of the buoyancy flux and the particle number flux in Lecce. When taking into account only near-neutral and unstable conditions ($z_e/L < 0.1$), there is no considerable change of the diurnal cycles of wind speed, air temperature, particle number concentration, friction velocity and buoyancy fluxes both in Lecce and in Innsbruck. However, particle number fluxes are slightly enhanced in Lecce compared to Fig. 3.

3.2 Spectral analysis by multiresolution decomposition

We use multiresolution decomposition (MRD) as a simple tool to calculate cospectra of the vertical wind speed w, temperature T, and particle number concentration C, respectively. The integrals of the MRD cospectra, as given by Eq. 8, represent the total covariances w'T' and w'C', i.e. the buoyancy and particle number fluxes. Due to the fact that the typical length scales of eddies increase with increasing height in the surface layer, it is common practice to investigate cospectra as a function of the normalized frequency $n = f z_e/u$, where f is the frequency [s^{-1}], z_e is the effective measurement height [m], and u is the horizontal wind speed [$m\ s^{-1}$] (e.g. Foken, 2008). To compare the contributions of different frequencies to the total flux, individual cospectra are normalized by the corresponding flux to yield the unit area normalized cospectral density. The normalized cospectra indicate the contributions of different frequencies to the buoyancy and particle number fluxes.

Comparing MRD cospectra in Lecce and Innsbruck

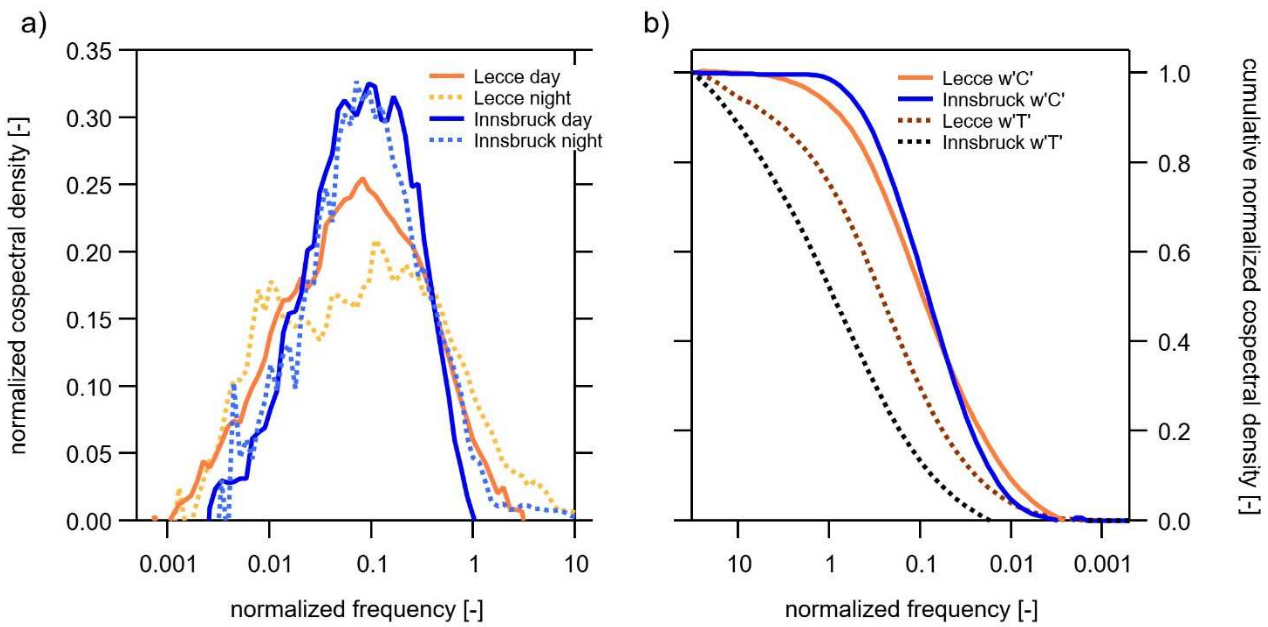

Fig. 4: a) Median normalized cospectra of particle number fluxes in Lecce (orange) and Innsbruck (blue) during daytime (11:00-17:00, solid) and night-time (23:00 – 05:00, dotted) conditions; b) cumulative median normalized cospectra of particle number fluxes (solid) and buoyancy fluxes (dotted) in Lecce and Innsbruck.

Figure 4a compares the median normalized cospectra of particle number fluxes measured in Lecce and Innsbruck during daytime conditions from 11:00 to 17:00, and during the night from 23:00 to 05:00. The location of the cospectral peak n_m is close to a value of $n_m = 0.085$, which is expected under neutral and unstable conditions (Kaimal et al., 1972). In Lecce, the median cospectrum at night is broader than during the day, with equal flux contributions in the normalized frequency range between 0.01 and 1. In Innsbruck, the cospectrum is narrower compared to Lecce, and very similar during daytime and night-time, indicating a narrower distribution of eddy sizes compared to Lecce. This indicates that the typical eddy size associated with the normalized frequency of the cospectral peak is more dominant in Innsbruck compared to Lecce, possibly due to a larger heterogeneity of the urban canopy in the flux footprint of Lecce compared to Innsbruck.

When comparing median cumulative cospectra in Lecce and Innsbruck (Fig. 4b), high frequency contributions are evidently higher for buoyancy fluxes than for particle number fluxes. There are no considerable contributions to particle number fluxes at normalized frequencies greater than 1, especially in Innsbruck. This illustrates the imperfect response of the particle counters to concentration fluctuations, while the sonic anemometer measurement fully resolves the acoustic temperature fluctuations at the measurement frequency. In contrast, low frequency contributions to buoyancy fluxes are much smaller than to particle number fluxes, indicating that scalar similarity of temperature and particle number concentration is limited. In summary, the particle flux cospectra are shifted to lower frequencies compared to the buoyancy flux cospectra, and the particle and buoyancy flux cospectra are more similar in Lecce than in Innsbruck. The same observations are found when separating daytime and night-time data.

Diurnal evolution of MRD cospectra

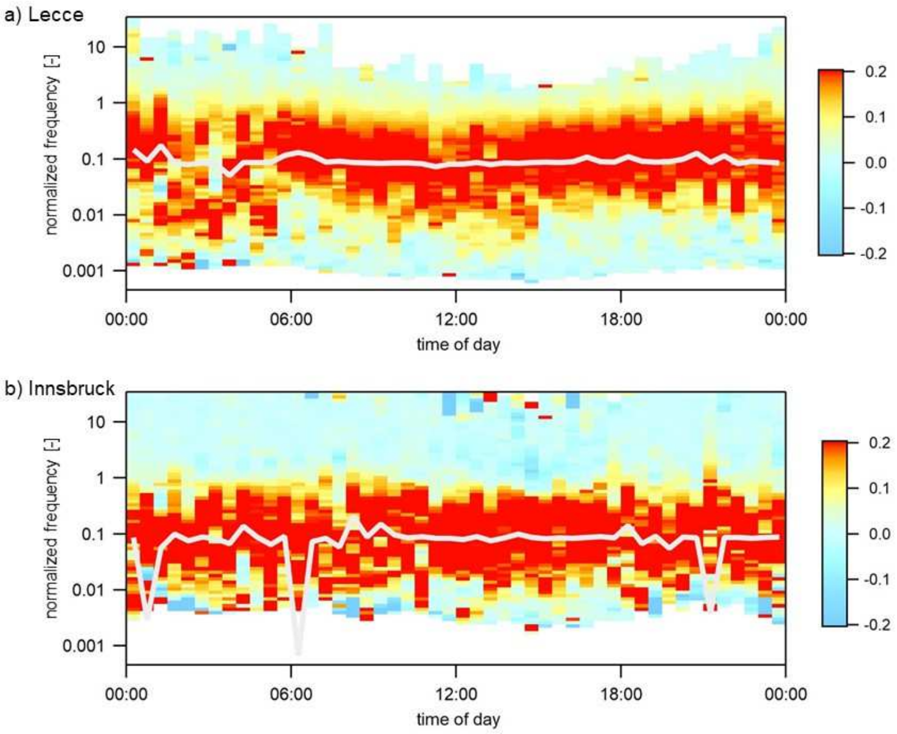

Figure 5: Diurnal cycle of median normalized particle number flux cospectra in a) Lecce and b) Innsbruck; the white line indicates the cospectral peak fitted to the median cospectra of all 30 min intervals.

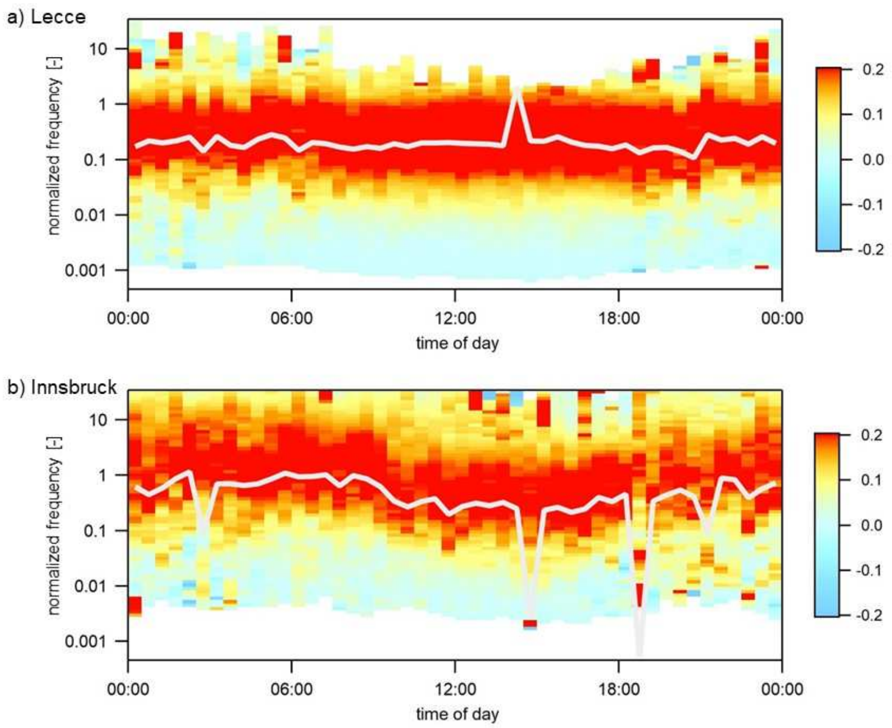

Figure 6: Diurnal cycle of median normalized buoyancy flux cospectra in a) Lecce and b) Innsbruck; the white line indicates the cospectral peak fitted to the median cospectra of all 30 min intervals.

Figures 5 and 6 show the diurnal evolution of the median normalized cospectra with respect to particle number fluxes and buoyancy fluxes in Lecce and Innsbruck obtained from multiresolution decomposition. The white line indicates the cospectral peak at the normalized frequency n_m fitted to the median cospectra of all 30 min intervals assuming a model for the normalized cospectrum Co according to Eq. 10 (e.g. Horst, 1997)

$$\mathrm{Co} = \frac{2}{\pi}\frac{n/n_m}{1+(n/n_m)^2} \tag{10}$$

Thus, the cospectral peak indicates the normalized frequency n with the highest contribution to the flux, i.e. the inverse of the dominant time scale of turbulent transport. The red colours indicate the normalized frequency ranges with the highest contribution to the total fluxes at different times of the day.

For particle number fluxes (Fig. 5), the main contributions are in the normalized frequency range from 0.01 to 1, both in Lecce and in Innsbruck. In Lecce (Fig. 5a), there is a lot of scatter from 00:00 to 06:00, when fluxes are generally small. In the morning after 06:00, there seems to be a slight shift from higher frequencies to lower frequencies around noon, and then again a slight increase to higher frequencies contributing to the particle number flux in the evening. In contrast, there is no obvious diurnal pattern in the median normalized cospectra of buoyancy fluxes (Fig. 6a), and the contributing frequencies are clearly shifted to higher frequencies from 0.1 to 1. In Innsbruck, there is no obvious diurnal pattern in the median normalized cospectra of particle number fluxes (Fig. 5b) but a shift from higher frequency contributions during night-time to lower frequency contributions to the buoyancy flux during the day (Fig. 6b). This indicates that the dominant time scales of turbulent transport are different for the two studied scalars, particle number concentration and temperature. The peak frequencies of the particle flux cospectra are similar in Lecce (median of n_m = 0.087) and in Innsbruck (median of n_m = 0.086), close to the expected value of n_m = 0.085, and relatively constant throughout the day (Lecce interquartile range 0.085-0.091; Innsbruck interquartile range 0.079-0.089). In contrast, the buoyancy flux cospectra show clearly higher peak frequencies (Lecce median of n_m = 0.193; Innsbruck median of n_m = 0.445) compared to the particle flux cospectra. The higher median value in Innsbruck is mostly due to much higher peak frequencies during the night-time. In the well-mixed convective boundary layer, the Eulerian integral scale Λ_i associated with the scalar flux is related to the normalized frequency of the cospectral peak, n_m, and the effective measurement height z_e according to Eq. 11 (Mann and Lenschow, 1994):

$$\Lambda_i = \frac{z_e}{2\pi n_m} \tag{11}$$

For the particle fluxes, this length scale is relatively stable with a median value of Λ_i = 13 m in Lecce and Λ_i = 45 m in Innsbruck. In contrast, the median Eulerian integral scale of the buoyancy fluxes is

Λ_i = 6 m in Lecce, and exhibits a diurnal cycle in Innsbruck with values around Λ_i = 6 m in the night-time and Λ_i up to 20 m during daytime. It should be noted that the effective measurement height in Innsbruck is z_e = 24.6 m, and z_e = 7 m in Lecce. Thus, both the ratio of the Eulerian integral scales of particle flux cospectra and the ratio of the effective measurement heights in Innsbruck and Lecce are approximately 3.5, and the different values of the Eulerian integral scale of particle flux cospectra are proportional to the different effective measurement heights above the two urban canopies.

3.3 Wavelet analysis

Wavelet analysis yields cross-wavelet spectra of particle number concentration and wind speed with information about the contributions of different frequency ranges of the turbulent time series to the total fluxes in both the time and frequency domains. This allows to analyse the typical contributions of different time scales, i.e. eddy sizes, in more detail.

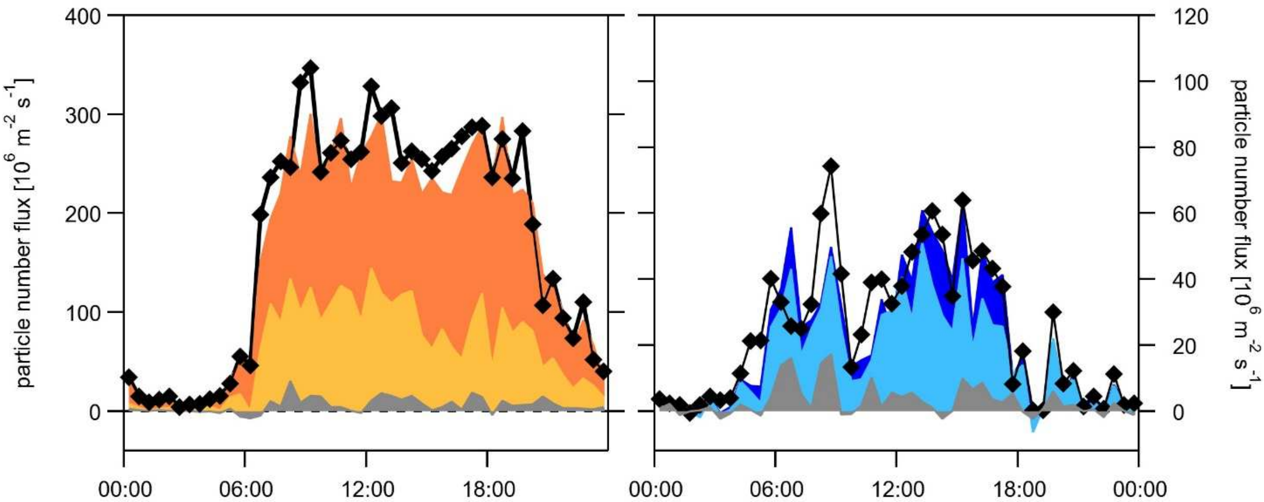

Figure 7: Median diurnal cycle of particle number fluxes reconstructed from wavelet analysis for 30 min intervals (black) in Lecce (left) and Innsbruck right); flux contributions of 2 – 20 s scales in orange and dark blue, 20 – 200 s scales in yellow and light blue, and 200 – 2000 s scales in grey.

Figure 7 shows the median diurnal cycle of 30 min particle number fluxes in Lecce and Innsbruck reconstructed from wavelet analysis, and the contributions of three different frequency ranges corresponding to time scales of 2 – 20 s (small eddy sizes), 20 – 200 s (medium eddy sizes), and 200 – 2000 s (larger eddy sizes). Note that the contributions of scales can be positive or negative, and therefore, the sum of the three frequency ranges may be slightly larger or smaller at any time interval. Interestingly, the 2 – 20 s time scales (orange) contribute very strongly to the particle flux in Lecce, while in Innsbruck the 20 – 200 s time scales (light blue) are clearly dominant. This is consistent with the smaller Eulerian integral scale of the particle fluxes in Lecce compared to Innsbruck (cf. section 3.2). Both in Lecce and Innsbruck, the contribution of the 200 – 2000 s time scales to the total median particle flux is very small, i.e. less than $20 \cdot 10^6$ m^{-2} s^{-1}. However, in many cases on individual days, quick changes in fluxes are due to larger-than-usual contributions of the 200 – 2000 s time scales. Thus, sporadically, larger eddies can contribute significantly to turbulent fluxes and may lead to sudden changes of the particle number concentration.

Taking advantage of the localization in the time domain, an estimate of the particle number flux can be calculated from cross-wavelet spectra not only for 30 min intervals (like in EC) but also for shorter time intervals, e.g. 1 min.

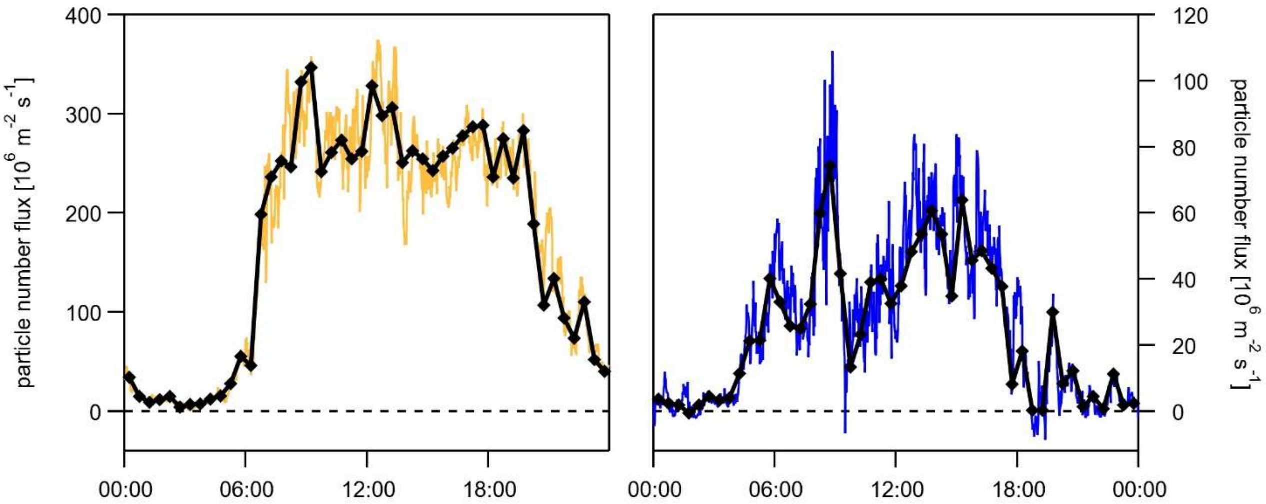

Figure 8: Median diurnal cycle of particle number fluxes reconstructed from wavelet analysis for 30 min intervals (black) and 1 min intervals (smoothed with a 30 min rolling average filter) in Lecce (left, orange) and Innsbruck (right, blue).

Figure 8 shows the median diurnal cycle of particle number fluxes in Lecce and Innsbruck, reconstructed from wavelet analysis based on 30 min intervals and 1 min intervals. Apparently, the 1 min flux estimates are scattered around the 30 min flux estimates with deviations of about 30 % during daytime. In Lecce, the deviations are quite small during the night and constant during the day. In Innsbruck, the strongest deviations occur in the transition periods of wind direction reversal, i.e. around 09:00 in the morning, and between 17:30 and 19:00 in the evening. During periods when the 1 min flux estimates are close to the 30 min flux estimates, steady state conditions are expected. However, this interpretation should not be applied to median diurnal cycles of the 1 min and 30 min wavelet flux estimates but to individual time periods of the Lecce and Innsbruck data sets.

Conclusions

On average, particle emission is dominant in both cities. The particle emission fluxes follow a similar diurnal cycle but are much stronger in Lecce compared to Innsbruck. The diurnal cycle of the particle number concentration shows three maxima in Lecce: one in the morning, one at noon and one in the late afternoon. In Innsbruck, only the morning and late afternoon maxima are visible. These two peaks are probably associated with high traffic density in the morning and evening rush hours, and the noontime peak in Lecce is likely due to local particle nucleation. The source areas for fluxes were estimated to be much smaller than those for concentrations. The fact that the flux source areas include the respective main roads located near the experimental sites, and that the diurnal cycle of particle emission fluxes is consistent with vehicular traffic activity, traffic is identified as a major emission source of particles both in Lecce and in Innsbruck.

Multiresolution decomposition allowed to compare the normalized cospectra of vertical wind speed and particle number concentration, and thus, the contribution of different frequencies to the total particle number flux. On the one hand, the shape of the median normalized cospectra of particle fluxes was slightly different in Lecce and Innsbruck, with a broader distribution of frequencies contributing to the flux in Lecce compared to Innsbruck, especially at night. On the other hand, the cospectral peak, i.e. the frequency with the largest contribution to the particle number flux, was similar in Lecce and in Innsbruck. The cospectral peak of particle fluxes was relatively constant throughout the day both in Lecce and Innsbruck, with a median value of 0.087 in Lecce and 0.086 in Innsbruck. The cospectral maximum is expected at $n_m = 0.085$ under neutral conditions. These findings support the assumption of spectral similarity for cospectra of urban particle number fluxes in two cities with different micrometeorological conditions. At the same time, scalar similarity with respect to temperature and particle number concentration is limited. However, when comparing cospectra of particle number fluxes and buoyancy fluxes, the scalars are more similar in Lecce than in Innsbruck; in both cities, the cospectral peak of the buoyancy fluxes is shifted to higher frequencies, and the contribution of high frequencies is larger to the buoyancy flux than to the particle flux. This may indicate that high frequency particle flux contributions were dampened due to insufficient time resolution of the condensation particle counters, even when using 1 Hz data in this study.

Considering the results of the wavelet analysis, full resolution of the high frequency contributions may be particularly important in Lecce, where the 2 – 20 s time scales contribute very strongly to the particle flux in Lecce, while in Innsbruck the 20 – 200 s time scales are clearly dominant. Both in Lecce and Innsbruck, the contribution of the 200 – 2000 s time scales to the total median particle flux is very small. Thus, in order to quantify particle emission fluxes in these two cities, the averaging interval used for the EC calculations may be changed to shorter periods of 5 or

10 min, and steady-state assumptions may not be required for full 30 min intervals. However, larger-sized eddies might sporadically contribute in a very strong way to particle number fluxes. Even if the steady state assumption is not fulfilled, reconstruction of flux estimates from wavelet analysis can still be applied to shorter time intervals. For the studied periods in Lecce and Innsbruck, the 1 min wavelet estimates of particle number fluxes deviated by less than 30 % from the 30 min EC flux estimates on average during daytime.

In summary, the presented results clearly suggest that spectral similarity of urban particle number fluxes holds to a large extent, even when comparing two very different urban environments such as Lecce close to the Adriatic Sea and Innsbruck in the Alpine Inn valley. The results also illustrate the great potential of spectral flux estimation methods such as wavelet analysis for application in future studies of turbulent particle fluxes.

Acknowledgements

The authors thank the University of Salento (in Lecce) for hosting the instruments in its premise. A special thanks to Dr. Antonio Donateo and Dr. F.M. Grasso (ISAC-CNR) for their help in the setup of the measurement campaign and in data collection in Lecce. The authors are grateful for the hospitality and support provided by T. Karl and M. Graus (University of Innsbruck), and the help by L. von der Heyden and M. Deventer in carrying out the particle number flux measurements during the Innsbruck Air Quality Study 2015. Part of this study was financially supported by the TU Berlin Office of International Affairs.

References

Arya, S.P., 1999. Air pollution meteorology and dispersion. Oxford University Press, New York, 310 pp.

Aubinet, M., Grelle, A., Ibrom, A., Rannik, Ü., Moncrieff, J., Foken, T.,Kowalski, A. S., Martin, P. H., Berbigier, P., Bernhofer, C., Clement, R., Elbers, J., Granier, A., Grünwald, T., Morgenster, K., Pilegaard, K., Rebmann, C., Snijders, W., Valentini, R., Vesala, T., 1996. Estimates of the Annual Net Carbon and Water Exchange of Forests: The EUROFLUX Methodology. Chapter in Advances in Ecological research, 112-175.

Aubinet, M., Vesala, T., Papale, D. (Eds.), 2012. Eddy Covariance. A practical guide to measurement and data analysis. Springer, Dordrecht, 438 pp.

Baldocchi, D. D., Bruce, B. H., Tilden, P. M., 1988. Measuring biosphereatmosphere exchanges of biologically related gases with micrometeorological methods. Ecology, 69(5), 1331-1340.

Burba, G., Schmidt, A., Scott, R. L., Nakai, T. Kathilankal, J. Fratini, G. Hanson, C. Law, B. McDermitt, D. K., Eckles, R. Furtaw, M., Velgersdyk, M., 2012. Calculating CO2 and H2O eddy covariance fluxes from an enclosed gas analyzer using an instantaneous mixing ratio. Global Change Biology, 18, 385-399.

Conte, M., Donateo, A., Dinoi, A., Belosi, F., Contini, D., 2015. Case study of particle number fluxes and size distributions during nucleation events in southeastern Italy in the summer. Atmosphere 6, 942–959.

Conte, M., Donateo, A., Contini, D., 2018. Characterisation of particle size distributions and corresponding size-segregated turbulent fluxes simultaneously with CO_2 exchange in an urban area. Sci. Total Environ. 622–623, 1067–1078.

Contini, D., Donateo, A., Elefante, C., Grasso, F.M., 2012. Analysis of particles and carbon dioxide concentrations and fluxes in an urban area: correlation with traffic rate and local micrometeorology. Atmos. Environ. 46, 25–35.

Deventer, M.J., von der Heyden, L., Lamprecht, C., Graus, M., Karl, T., Held, A., 2018. Aerosol particles during the Innsbruck Air Quality Study (INNAQS): Fluxes of nucleation to accumulation mode particles in relation to selective urban tracers. Atmospheric Environment, 190, 376-388.

Dorsey, J.R., Nemitz, E., Gallagher, M.W., Fowler, D., Williams, P.I., Bower, K.N., Beswick, K.M., 2002. Direct measurements and parameterization of aerosol flux, concentration and emission velocity above a city. Atmos. Environ. 36, 791-800.

Foken, T., Wichura, B., 1996. Tools for quality assessment of surface-based flux measurements. Agricultural and Forest Meteorology, 78, 83-105.

Foken, T., 2008. Micrometeorology. Springer, Heidelberg, 308 pp.

Grimmond, C.S.B., Oke, T.R., 1999. Aerodynamic properties of urban areas derived from analysis of surface form. J. Appl. Meteorol. 38, 1262–1292.

Horst, T.W., 1997. A simple formula for attenuation of eddy fluxes measured with first order-response scalar sensors. Bound.-Layer Meteorol. 82, 219–233.

Howell, J.F., Mahrt, L., 1997. Multiresolution flux decomposition. Boundary-Layer Meteorol., 83, 117–137.

Kaimal, J. C.,Wyngaard, J. C., Izumi, Y., and Cote, O. R., 1972. Spectral characteristics of surface-layer turbulence. Quart. J. Roy. Meteorol. Soc. 98, 563–589.

Karl, T., Gohm, A., Rotach, M.W., Ward, H.C., Graus, M., Cede, A., Wohlfahrt, G., Hammerle, A., Haid, M., Tiefengraber, M., Lamprecht, C., Vergeiner, J., Kreuter, A., Wagner, J., Staudinger, M., 2020. Studying Urban Climate and Air quality in the Alps - The Innsbruck Atmospheric Observatory. Bulletin of the American Meteorological Society 101, E488–E507. https://doi.org/10.1175/BAMS-D-19-0270.1

Katul, G.G., Parlange, M.B., 1995. Analysis of land surface heat fluxes using the orthonormal wavelet approach. Water Resources Research 31, 2743-2747.

Kljun N., Rotach, M.W., Schmid, H.P., 2002. A three-dimensional backward Lagrangian footprint model for a wide range of boundary-layer stratifications. Boundary-Layer Meteorology, 103, 205–226.

Longley, I.D., Gallagher, M.W., Dorsey, J.D., Flynn, M., 2004. A case-study of fine particle concentrations and fluxes measured in a busy street canyon in Manchester, UK. Atmos. Environ. 38, 3595-3603.

Mann, J. and Lenschow, D. H., 1994. Errors in airborne flux measurements. J. Geophys. Res. 99, 14519–14526.

Mårtensson, E.M., Nilsson, E.D., Buzorius, G., Johannsson, C., 2006. Eddy covariance measurements and parameterization of traffic related particle emissions in an urban environment. Atmos. Chem. Phys. 6, 769-785.

Martin, C.L., Longley, I.D., Dorsey, J.R., Thomas, R.M., Gallagher, M.W., Nemitz, E, 2009. Ultrafine particle fluxes above four major European cities. Atmos. Environ. 43,4714-4721.

McMillen, R. T., 1988. An eddy correlation technique with extended applicability to non-simple terrain. Boundary-Layer Meteorology, 43, 231-245.

Moncrieff, J. B., Malhi, Y., Leuning, R., 1996. The propagation of errors in long-term measurements of land-atmosphere fluxes of carbon and water. Global Change Biology, 2, 231-240.

Nemitz, E., Fowler, D., Dorsey, J.R., Theobald, M.R., McDonald, A.D., Bower, K.N., Beswick, K.M., Williams, P.I., Gallagher, M.W., 2000. Direct measurements of size-segregated particle fluxes above a city. J. Aerosol. Sci. 31(2), 116-118.

Reynolds, O., 1894. On the dynamical theory of turbulent incompressible viscous fluids and the determination of the criterion. Phil. Trans. R. Soc. London A, 186, 123-161.

Saito, M. and Asanuma, J., 2008. Eddy covariance calculation revisited with wavelet cospectra. Sola, 4, 49-52, doi:10.2151/sola.2008- 013, 2008.

Schaller, C., Göckede, M., and Foken, T., 2017. Flux calculation of short turbulent events – comparison of three methods. Atmos. Meas. Tech., 10, 869–880, https://doi.org/10.5194/amt-10-869-2017.

Schmid, H.P., Oke T.R., 1990. A model to estimate the source area contributing to turbulent exchange in the surface layer over patchy terrain. Quarterly Journal of the Royal Meteorological Society, 116, 965-988.

Schmid, H.P., 1994. Source areas for scalars and scalar fluxes. Boundary-Layer Meteorol. 67, 293–318.

Toda, M. and Sugita, M., 2003. Single level turbulence measurements to determine roughness parameters of complex terrain. Journal of Geophysical Research, Atmospheres, 108, NO. D12, 4363.

Torrence C, Compo GP (1998) A practical guide to wavelet analysis. Bull Am Meteorol Soc 79:61–78

van den Kroonenberg, A., Bange, J., 2007. Turbulent flux calculation in the polar stable boundary layer: multiresolution flux decomposition and wavelet analysis. J. Geophys. Res., 112, D06112, doi:10.1029/2006JD007819.

Vesala, T., Kljun, N., Rannik, U., Rinne, J., Sogachev, A., Markkanen, T., Sabelfeld, K., Foken, Th., Leclerc, M.Y., 2008. Flux and concentration footprint modelling: state of the art. Environ. Pollut. 152, 653

von der Heyden, L., Deventer, M.J., Graus, M., Karl, T., Lamprecht, C., Held, A., 2018. Aerosol particles during the Innsbruck Air Quality Study (INNAQS): The impact of transient fluxes on total aerosol number exchange. Atmospheric Environment, 190, 389-400.

Graphical abstract